J. exp. Biol. ***188****, 65–88 (1994)*
Printed in Great Britain © The Company of Biologists Limited 1994

THE POSITION-DEPENDENT NATURE OF POSTURAL RESISTANCE REFLEXES IN THE LOCUST

L. H. FIELD AND M. M. L. COLES
Department of Zoology, University of Canterbury, Christchurch 1, New Zealand

Accepted 15 November 1993

Summary

The resistance reflexes of tibial extensor and flexor muscles, of all six legs in the locust, show changes in gain at different femur–tibia angles (FTA). In all muscles the gain is high for small angles (near full flexion) and low for large angles (near full extension, approximately 160 °). An exception occurs in the mesothoracic flexor muscle, which shows two modes: one as above and another in which maximum gain occurs at 100–120 ° FTA.

The position-dependent character is evident at each stage of the reflex pathway: motor neurone, non-spiking interneurone and femoral chordotonal organ (the afferent source of the reflex). We conclude that position-dependency originates from a decrease in the number of phasic femoral chordotonal organ neurones sensitive to joint movement as larger FTAs are approached.

Position-dependency is only roughly correlated with the postural FTAs most commonly observed in the meso- and metathoracic legs of unrestrained resting locusts; no such correlation was evident for prothoracic legs. We propose that the major role of position-dependency is to allow resistance reflexes efficiently to counter torque introduced onto the femur–tibia joint by perturbations in the horizontal plane when the insect rests on a horizontal substratum and in the vertical plane when it rests on a vertical substratum.

Introduction

The resistance reflex is a negative feedback reflex generated in response to passive (non-voluntary) flexion or extension of an arthropod joint. Proprioceptive feedback from chordotonal organs in the joint excites motor neurones innervating muscles that resist the imposed movement and inhibits motor neurones innervating muscles that assist the movement (Bush, 1962). For example, forced flexion of the locust femur–tibia joint results in excitation of the extensor tibiae motor neurones and inhibition of the flexor tibiae motor neurones of the hind leg (Burrows and Horridge, 1974; Field and Burrows, 1982). This reflex provides postural stability against gravity and sporadic environmentally induced perturbations of stance.

Resistance reflexes have been described in all of the major leg joints of insects (Wilson, 1965; Bässler, 1972; Wright, 1976) and of decapod crustaceans (Bush, 1962, 1965). In

Key words: resistance reflex, posture, chordotonal organ, locust, proprioception, *Locusta migratoria*.

most cases, the reflexes are mediated by chordotonal organ stretch receptors located in each joint (Wright, 1976).

In insects, the femoral chordotonal organ (FCO) mediates resistance reflexes in the tibial extensor and flexor muscles, which are the major muscles used in walking. The FCO spans the femur–tibia joint of each leg. It is anchored to the cuticle in the femur, and it is connected to the tibia by a cuticular apodeme which is pulled (stretching the FCO) as the tibia is flexed (Field and Burrows, 1982). The FCO typically contains from about 90 (metathoracic) to several hundred (prothoracic and mesothoracic) sensory neurones which collectively signal position, velocity, acceleration and direction of movement (Usherwood *et al.* 1968; Burns, 1974; Field and Rind, 1977, 1980; Hofmann *et al.* 1985; Field and Pflüger, 1989; Matheson and Field, 1990; Matheson, 1990). All angles of joint movement are encoded (Zill, 1985), although there is range fractionation within the sensory neurone population (Burns, 1974; Matheson, 1990, 1992; Field, 1991).

Because the FCO monitors movement at all femur–tibia angles, one may consider, *a priori*, that the resistance reflex response to a small arc of movement about a joint should be of equal strength, regardless of where that arc occurred in the total range of joint movement. Several authors have noted, however, that the strength of the reflex appears to vary with the position of joint movement. Bush (1962) first described this 'position effect' in the resistance reflexes of the walking legs of the crab *Carcinus maenas*. He showed that the reflex response of the opener/stretcher motor neurone and the 'slow' closer motor neurone varied with the position of the dactylus as it was passively moved. In the crab *Cardisoma guanhumi*, the reflexes increase in strength as imposed leg movements approach extreme joint positions (Spirito *et al.* 1972). In the locust, the resistance reflex of the metathoracic slow extensor tibiae (SETi) motor neurone decreases in strength with increasing femur–tibia angle (Field and Burrows, 1982). In the stick insect, similar observations have been made for muscles of the femur–tibia and coxo-trochanteral joints (Bässler, 1965; Schmitz, 1985).

The initial aim of the present study was to determine the extent of position-dependency in the strength of the resistance reflex of the extensor and flexor tibiae muscles of all three pairs of legs in the locust. Having demonstrated the generality of position-dependency, we then examined its origins in motor neurones, non-spiking interneurones and the FCO. Next, we sought to establish the physiological role(s) for position-dependency of reflex action by investigating the postural deployment of the three pairs of legs when animals were at rest. To this end, we recorded femur–tibia angles in the legs of locusts at rest on horizontal and vertical substrata and determined whether the preferred leg angles matched the peaks in position-dependency in plots of resistance reflex strength against joint angle. Finally, we modelled the mechanics of the femur–tibia joint to show how position-dependency of resistance reflexes could counteract unfavourable muscle lever advantages that occur at some joint settings in horizontal and vertical postures.

Materials and methods

Adult locusts [*Locusta migratoria* (L.)], maintained in crowded cultures at 25 ˚C, were used in all experiments.

Physiological recordings

Myogram experiments

Myograms were recorded from the extensor or flexor tibiae muscles by inserting fine copper leads through pinholes made in the overlying cuticle. Optimal recording sites were initially located by implanting leads at various positions above the muscles; the sites with least cross-talk from antagonist muscles were used in all subsequent experiments. Under the conditions used (see below), the myograms represented slow motor neurone activation of the muscles. The signals were amplified, displayed, stored on magnetic tape and printed using conventional equipment. All spikes were counted within each reflex burst during the appropriate direction of tibial movement.

Tibial movement was achieved by immobilising a locust on a Plasticine platform with the chosen tibia free to move, and attaching a light rod (2 mm×150 mm) to the tibia by cotton thread and a low-melting-point vinyl/wax mixture. The rod was moved longitudinally in a horizontal plane (see next paragraph) by a backlash-free motor drive (adapted from a portable tape recorder) to provide a sinusoidal push–pull movement. This movement was monitored by a photocell which detected the path of a light beam that was interrupted by a flag mounted on the driving rod. The resulting tibial movement imposed a longitudinal length change upon the FCO through its distal apodeme. The metathoracic FCO length varies nearly linearly with femur–tibia angle (FTA) in the range 0–120 ˚ (Field and Burrows, 1982), but beyond about 140 ˚ the proximal end of the apodeme moves transversely, causing a twist in the strap-like FCO ligament (Field, 1991), as well as a complex distortion of the FCO body. Although the length change imposed on the FCO at tibial angles greater than 120 ˚ is neither sinusoidal nor linear, it clearly stimulates a population of velocity-sensitive chordotonal organ neurones which increase their firing rate as the tibia extends through these large FTAs.

The horizontal travel of the rod could be adjusted to provide a 20 ˚ arc of tibial movement for each leg tested. Different 20 ˚ arcs within the range 20–160 ˚ of femur–tibia angle were achieved by using a micrometer drive to displace the preparation platform forwards or backwards along the length of the rod, thus altering the rest FTA. All reflex tests were carried out at a driving frequency of 1 Hz.

The protocol of each experiment was to deliver 20 cycles of joint movement (20 ˚ arcs) at the smallest angle (20–40 ˚), to rest for 30 s at the midpoint of the arc, and then to move to the next 20 ˚ arc and repeat the 20-cycle stimulus. In the metathoracic leg, the arcs used were 20–40 ˚, 60–80 ˚, 100–120 ˚ and 140–160 ˚. In the prothoracic and mesothoracic legs, an arc of 30–50 ˚ was used instead of 20–40 ˚, because of difficulties in achieving uniform leg movement at 20 ˚. The sequence of arcs was randomly reversed to control for cumulative effects on reflex strength. Fifty-two locusts were used for myogram reflex experiments.

Intracellular experiments

Intracellular recordings were made from the somata of the metathoracic tibial extensor and flexor motor neurones and from non-spiking interneurones involved in the reflex pathway, by using glass microelectrodes filled with 2 mol l^{-1} potassium acetate (tip

resistances 30–50 MΩ). Locusts were mounted ventral side up, the ganglion was exposed and mounted on a wax-coated steel platform and the tracheal supply was left intact to allow the ganglion to be adequately supplied with oxygen. The ganglion was initially treated with a 0.1 % (w/v) solution of protease (Sigma type XIV) for 1–2 min, then bathed with a steady flow of saline at 20 °C. In these experiments, the FCO apodeme was exposed and stimulated directly, rather than through tibial movement as in the previous experiments. The FCO apodeme was grasped by micro-forceps mounted on an electromagnetic vibrator that was moved with a triangular waveform in an open-loop configuration, as described in Field and Burrows (1982) and Matheson (1990). The apodeme displacement was pre-calibrated against FTA. Motor neurones were identified by comparing their activity with spikes recorded extracellularly in flexor and extensor muscles. Non-spiking interneurones were characterised by the criteria described by Burrows (1979) and Burrows *et al.* (1988). Thirteen locusts were used for intracellular experiments.

Leverage experiments

To test muscle leverage at different FTAs, locusts were immobilised ventral side up, the thoracic ganglia were exposed and platinum hook stimulating electrodes were placed on the appropriate motor nerve near its junction with the ganglion. The nerve was pinched proximal to the electrode site. The electrodes were insulated from the surrounding tissues with Vaseline. All muscle nerves were stimulated at 40 Hz, except that of the metathoracic tibial extensor, which was stimulated at 20 Hz. Tetanic contractions were produced in each case and stimulation was continued until the force reached a stable plateau. The torque exerted on the tibia by tetanic contraction at different FTAs was measured with a Grass FT03 force gauge (which was always attached 2 mm from the distal end of the tibia, normal to the tibial axis). Fourteen locusts were used for the leverage experiments. Calculations of theoretical leverage of each muscle at the femur–tibia joint were made by measuring distances and angles of appropriate parts of the joint from drawings of legs. The legs were treated with 10 % KOH to dissolve the muscles, cleared and stained with lactophenol/Lignin Pink and drawn using a *camera lucida* on a Wild M.5 dissecting microscope at 30× magnification.

Behavioural observations

Femur–tibia angles of the pro-, meso- and metathoracic legs were measured in locusts at rest on the horizontal and vertical sides of their cages. A telescope and protractor were used to estimate leg angles optically from a viewing axis normal to the leg being measured. In all cases, measurements were taken after walking locusts had come to rest and settled. The settling process usually took several seconds. Locusts were not used if any contact or apparent interference had occurred during stopping and settling. Daily measurements were made from a population of approximately 400 locusts in four cages. Individuals were measured only once per day by systematically shifting observations across the cages. For horizontal postures N=293 locusts and for vertical postures N=309 locusts.

Results

Resistance reflexes

The myogram records allow an insight into which of the motor neurones to each muscle was activated during the resistance reflexes elicited under our experimental conditions. The tibial extensor muscles of the three pairs of legs receive two excitatory motor axons: the fast and slow extensor tibiae, FETi and SETi (Hoyle, 1978). In the pro- and mesothoracic muscles both units appeared to fire (Fig. 1A,B), whereas in the metathoracic extensor only SETi fired (the much larger FETi spike only occurred at higher movement velocities) (Fig. 1C). The flexor tibiae muscle receives at least nine excitatory motor axons: three slow, three intermediate and three fast (Hoyle, 1978). These nine neurones form three groups within the ganglion (anterior, posterior, lateral): each group contains a fast, a slow and an intermediate motor neurone. In our experiments, the prothoracic flexor usually received excitation from one or two slow units (Fig. 1D) but the mesothoracic flexor often received reflex excitation from several slow units (Fig. 1E). Reflex activity in the metathoracic flexor was usually limited to one (Fig. 1F) or two slow units during movement at 1 Hz. More rapid tibial movement (not shown) demonstrated that larger spikes of intermediate and fast flexor units are only recruited above 1 Hz.

The strength of the resistance reflex was position-dependent in both the extensor and flexor muscles of all legs. However, the nature of position-dependency differed between legs for a given muscle (Fig. 2). In the prothoracic legs, the reflex was strongest at the smallest angle and steadily decreased with increasing joint angle until it reached

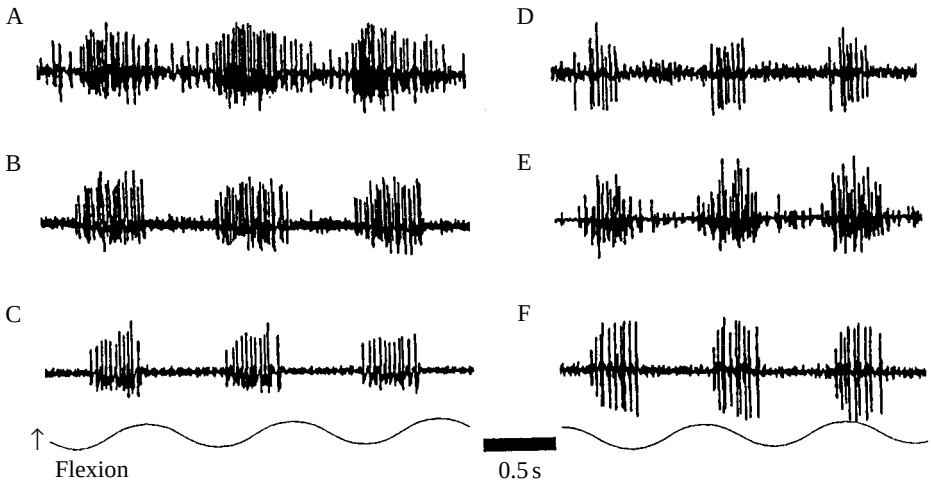

Fig. 1. Myogram recordings from the six leg muscles studied. Resistance reflex responses are to 1 Hz sinusoidal movement of the femur–tibia joint through 20 ° arcs. Although the motor units tended to facilitate, making single units difficult to identify, it was clear that they were primarily units with low-velocity thresholds and were therefore mostly slow units. At higher movement velocities, much larger units could be recruited. (A) Prothoracic extensor. (B) Mesothoracic extensor. (C) Metathoracic extensor (SETi only). (D) Prothoracic flexor. (E) Mesothoracic flexor. (F) Metathoracic flexor.

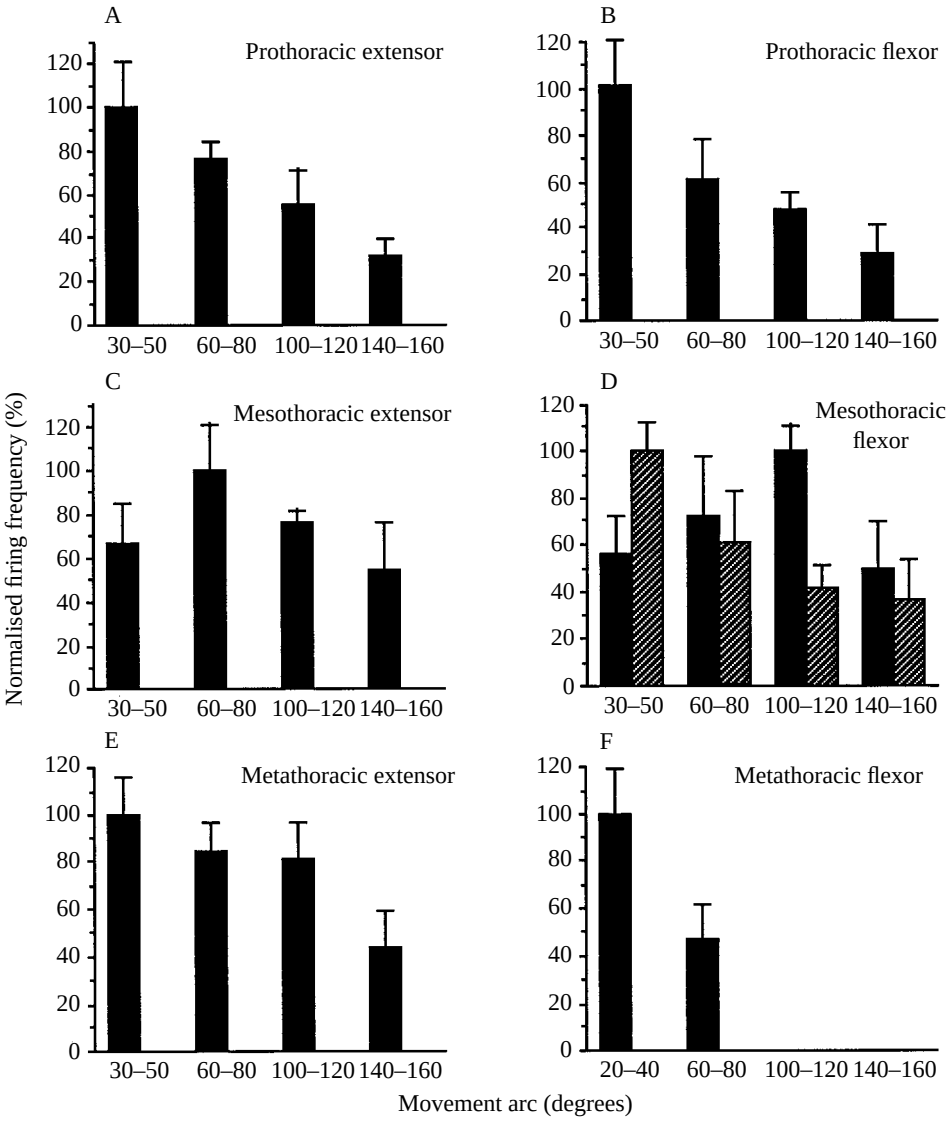

Fig. 2. Position-dependent changes in resistance reflex gain in the extensor (A,C,E) and flexor (B,D,F) muscles of the pro-, meso- and metathoracic legs. Movement of the tibia over 20 ˚ arcs evokes the highest firing frequencies at flexed angles, except in the mesothoracic flexor, which showed one or other of two consistently different patterns (hatched bars and filled bars). In all histograms, ten bursts of spikes were counted for each arc from records such as those in Fig. 1. Firing frequencies (spikes s^{-1}) were first normalised and then plotted as mean + S.D. The numbers of locusts used were as follows: prothoracic extensor, 5; prothoracic flexor, 8; mesothoracic extensor, 4; mesothoracic flexor, 14; metathoracic extensor, 11; metathoracic flexor, 4.

approximately one-third of its maximum strength. At each position, the relative reflex strength was reasonably consistent between animals as indicated by the small standard

deviations. The position-dependency plots for the prothoracic extensor and flexor tibiae muscles were very similar in form (Fig. 2A,B).

The reflexes of the mesothoracic extensor and flexor tibiae muscles showed different position-dependent peaks from those of the prothoracic legs (Fig. 2C,D). For the mesothoracic extensor muscle, the peak reflex strength occurred at 60–80 °, and the middle angles yielded greater reflex strengths than did the extreme angles (Fig. 2C). The mesothoracic flexor muscle showed two different trends in position-dependence (Fig. 2D). In eight of fourteen animals (hatched bars in Fig. 2D), the peak reflex strength occurred at 30–50 ° and decreased with increasing femur–tibia angle (as observed for the prothoracic muscles). In the remaining six animals, the peak reflex strength occurred at 100–120 °, with decreases towards both extremes of joint angle (filled bars in Fig. 2D). In both trends, the minimum reflex strengths (spike frequency) were 33–50 % of those observed at the peaks.

In the metathoracic leg, the peak reflex strengths of both extensor and flexor tibiae muscles occurred at 20–40 ° and decreased with increasing angle. The position-dependency of the extensor muscle was less marked than that of the pro- or mesothoracic muscles (Fig. 2E), whereas the flexor muscle showed a much greater dependency than that observed for any other muscle (Fig. 2F). This is underscored by the observation that no resistance reflexes were recorded for the flexor muscle at the 100–120 ° or 140–160 ° positions.

Intracellular recordings from the metathoracic SETi motor neurone confirmed the position-dependent nature of reflex excitation during joint flexion (Fig. 3A). During movement in the 50–30 ° arc, the neurone was rapidly depolarised and spiked at about 20 Hz. The rate of initial depolarisation and the spike frequency decreased (e.g. 16 Hz, 12 Hz) for movements in the 90–70 ° and 130–110 ° arcs, respectively. The mean peak of depolarisation (Fig. 3B) decreased by about 56 % between stimulation at 50–30 ° and at 130–110 ° for the 10 neurones sampled.

Intracellular recordings from a metathoracic slow flexor tibiae motor neurone of the anterior group (Fig. 3A) revealed a marked decrease in both depolarising excitation, and the preceding hyperpolarisation, as the arc moved from 30–50 ° (strong excitation) to 70–90 ° (only a single spike). Furthermore, the neurone was not depolarised during movements from 110 to 130 °, which confirms the absence of a resistance reflex at these angles for the metathoracic flexor tibiae muscle (see Fig. 2F). Intracellular recordings from other metathoracic flexor and extensor tibiae motor neurones all showed the same trend in position-dependency of the resistance reflex related to joint angle, with the maximum reflex depolarisation occurring at the smallest angle (Fig. 3B).

Non-spiking interneurones, which are known to mediate the flexor and extensor resistance reflexes (Burrows *et al.* 1988), also showed position-dependency in response to FCO input. In one example (Fig. 4A), a 5 mV sustained hyperpolarisation occurred during a movement in the 50–30 ° arc, and lasted during the return arc of 30–50 °. The effect was weak at 90–70 ° and was absent during the movement in the 130–110 ° arc. Five of the twelve non-spiking interneurones studied gave depolarising rather than hyperpolarising responses to FCO movement but, invariably, in all non-spiking interneurones, the response strength decreased as the femur–tibia angle increased (e.g. Fig. 4B).

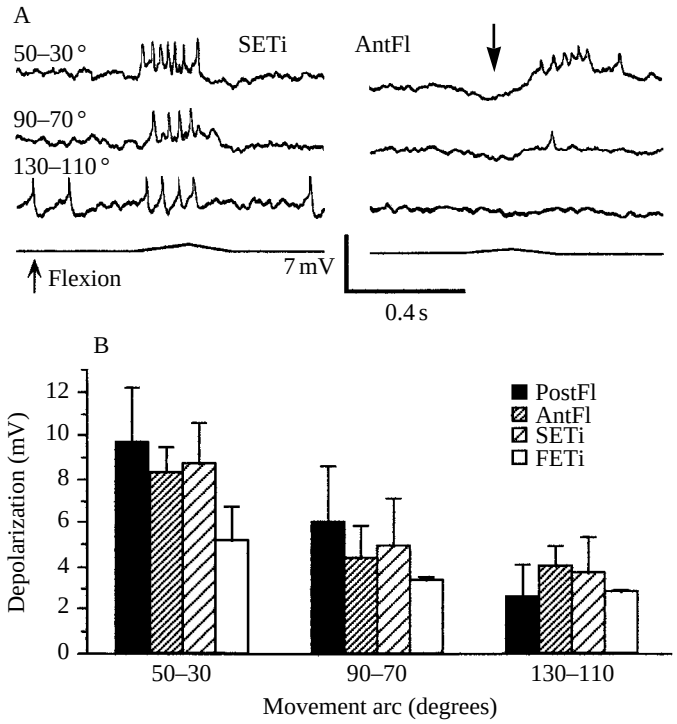

Fig. 3. Resistance reflex responses of motor neurones to femoral chordotonal organ (FCO) stimulation equivalent to 20° arcs of tibial movement. (A) Intracellular recordings of the metathoracic extensor (SETi) and an anterior flexor (AntFl) motor neurone. FCO stretch (equivalent to tibial flexion), indicated by upward movement in the bottom trace, produces a depolarisation and spikes in SETi but hyperpolarises (arrow) an anterior flexor (AntFl). Tibial extension produces the opposite response in both motor neurones. Both responses decrease with larger femur–tibia angles (FTAs) in both motor neurones. (B) Mean peak depolarisation (+S.D.) for tibial flexor and extensor motor neurones decreases as the 20° arc of FCO stimulation changes from small to large FTAs. PostFl, posterior flexor motor neurone (*N*=5 cells); Antfl, anterior flexor motor neurone (*N*=11 cells); SETi, slow extensor tibiae motor neurone (*N*=10 cells); FETi, fast extensor tibiae motor neurone (*N*=6 cells).

Recordings from the FCO nerve (made using hook electrodes in the metathoracic femur) allowed us to test whether the position-dependency of tibial resistance reflexes originated on the afferent side of the reflex. Spike sizes and firing frequencies were greatest during movement in the 50–30° arc and decreased with increasing FTA (Fig. 5A). The mean firing frequency for the whole nerve during movements over 130–110° was 56 % less than that observed during the 50–30° arc in the five sense organs tested (Fig. 5B).

Behavioural measurements

The femur–tibia angles of resting locusts were measured to determine whether peak resistance-reflex strength was related to the preferred leg angles of locusts resting on

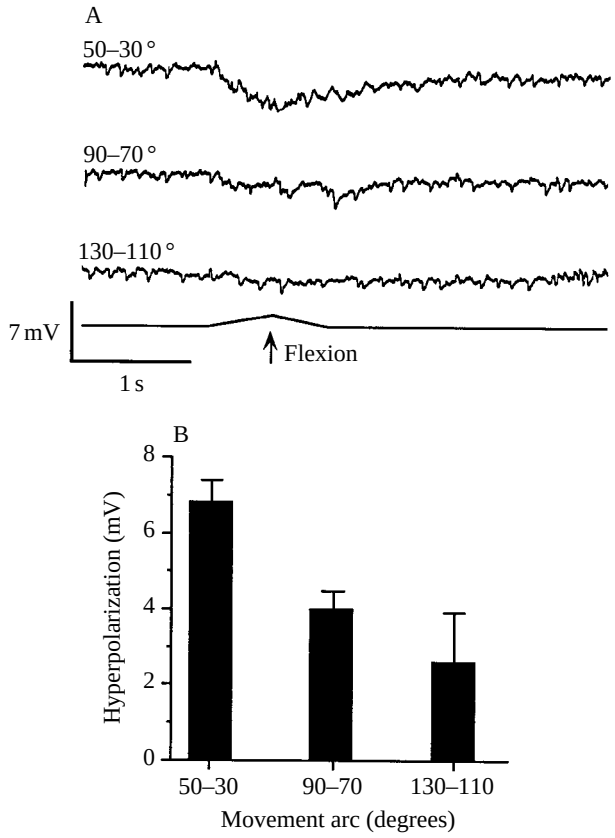

Fig. 4. Position-dependency in responses of metathoracic non-spiking interneurones to metathoracic FCO stimulation. (A) Intracellular recording showed a hyperpolarising response to FCO stretch (tibial flexion) at 50–30 °, but almost no response at 130–110 °. FCO movement is shown in the bottom trace. (B) Mean (+S.D.) response of four non-spiking interneurones, all of which showed smaller hyperpolarizations in response to FCO stimulation as the position of the arc increased.

horizontal and vertical substrata. The distributions of observed angles for locusts on the horizontal substratum are shown in the filled columns in Fig. 6. The distributions for all three pairs of legs were significantly different from the null hypothesis of no preferred leg angle (chi-squared; $P<0.01$). For the prothoracic legs, the peak occurred at 90–100 °, with 50 % of the observed angles falling between 80 and 120 ° (Fig. 6A). Similarly, the peak for the mesothoracic legs was at 90–100 °, and 50 % of the observations fell between 80 and 110 ° (Fig. 6B). A weakly bimodal distribution was found for the metathoracic leg (Fig. 6C): one peak was at 0–10 ° and a second peak occurred at 40–50 °. The total range of angles was decreased (0–100 °) compared with that for the pro- and mesothoracic legs (30–150 °).

Locusts facing upwards on a vertical substratum showed little change in preferred leg angle for the pro- and mesothoracic legs, but a marked change for the metathoracic leg

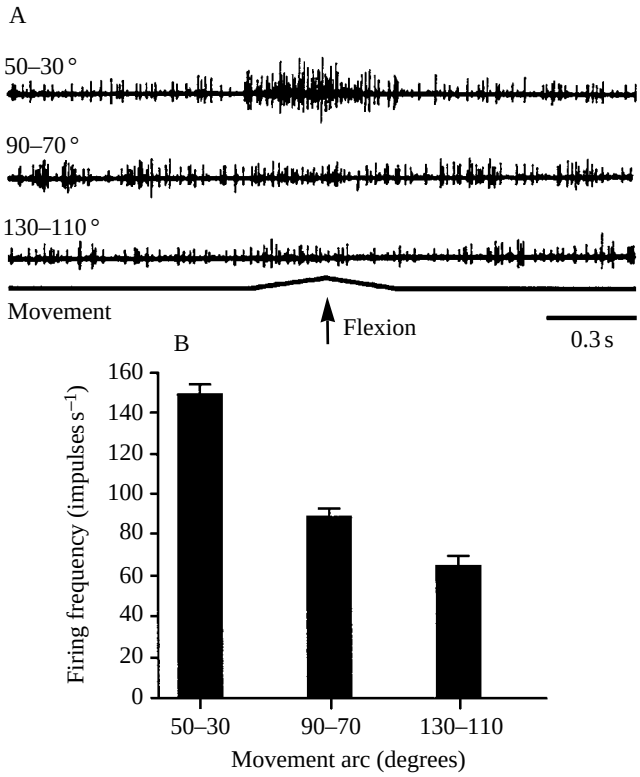

Fig. 5. Position dependency in the afferent discharge of the FCO. (A) Extracellular recordings from the FCO nerve during stimulation of the intact metathoracic FCO by tibial movement over 20 ˚ arcs. (B) Mean (+S.D., *N*=5) firing frequencies of all active neurones in the FCO from whole nerve recordings during linear movement in both directions.

(open bars in Fig. 6). In the prothoracic leg, there was a slight shift towards larger angles (median 90–100 ˚ for horizontal; 100–110 ˚ for vertical), but the peak remained at 90–100 ˚. In the mesothoracic leg, the distribution shifted towards smaller joint angles (median 80–90 ˚ for horizontal; 70–80 ˚ for vertical). In the metathoracic leg, 75.6 % of the observations occurred at 0–10 ˚ (compared with 16 % for locusts on a horizontal substratum), but the shape of the remaining distribution was similar to that for data from the horizontal substratum. When the metathoracic tibia was highly flexed, the tarsus was often folded against the tibia and was not in contact with the substratum (i.e. the leg did not support weight).

Muscle leverage experiments

Because Heitler (1974) predicted that the leverage of the metathoracic extensor muscle (of *Schistocerca gregaria*) should vary sinusoidally with FTA, we considered whether the variation in strength of the resistance reflex might reasonably act to compensate for loss of leverage at extreme joint angles in all legs. To answer this question, it was first necessary to describe the mechanics of the flexor and extensor muscles in all three pairs of

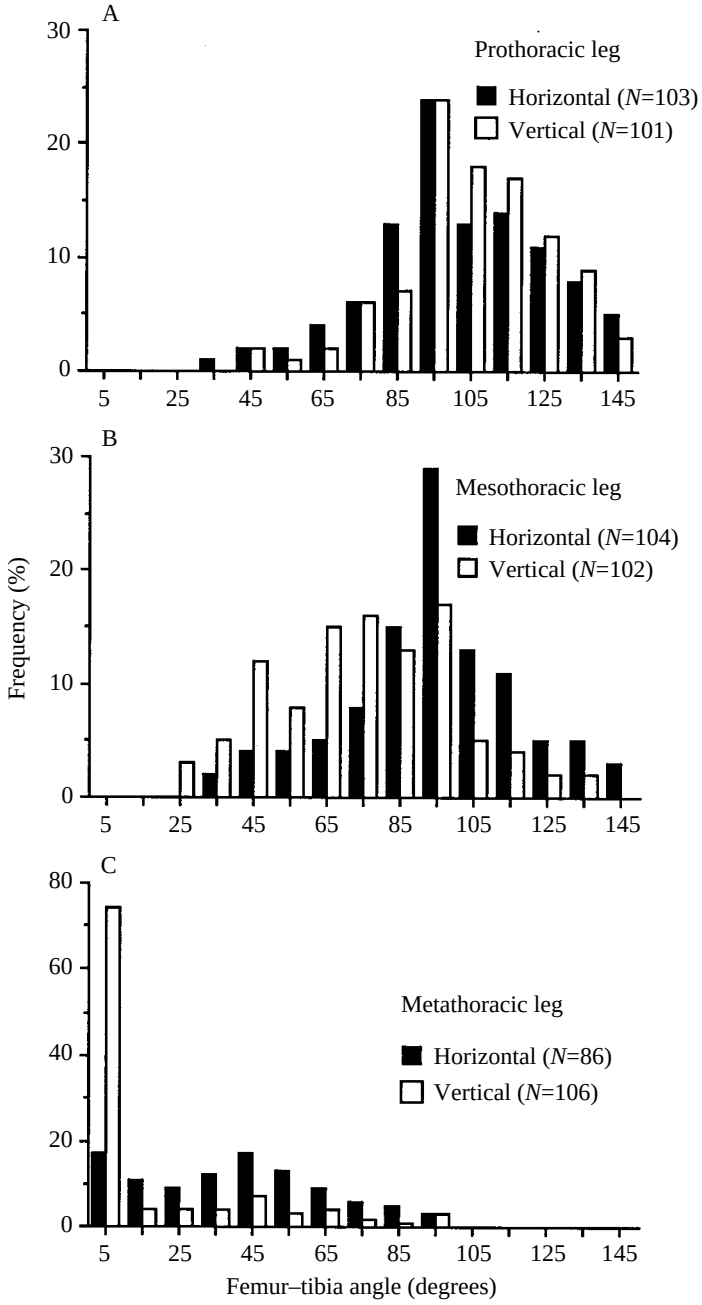

Fig. 6. Distributions of femur–tibia leg angles for locusts resting on a horizontal (filled bars) or vertical substratum (open bars). (A) Prothoracic leg. (B) Mesothoracic leg. (C) Metathoracic leg.

Locusta legs. This allowed us to predict how leverage should vary with FTA at each tendon insertion. We tested these predictions by measuring the torque developed at tetanic tension by the six muscles as FTA was varied. Finally, the muscle tension profiles were compared with the resistance reflex profiles illustrated in Fig. 2.

The femur–tibia joints of the pro- and mesothoracic legs had similar anatomy, in which the lever moment arms for the extensor tendons were offset from the tibial axis by 23.2±9.6 ° and 34.4±8.9 °, respectively, whereas the moment arms for the flexor tendons were nearly co-axial with the tibial axis (4.4±3.6 ° and 0.2±2.5 °, respectively) (Fig. 7A,C). In the metathoracic leg, the extensor moment arm was offset by a mean of 24.4±8.1 ° and the mean offset of the flexor moment arm was 50.0±4.7 ° (Fig. 7B,C). In addition, the metathoracic flexor tendon slides over Heitler's lump (Fig. 7B), which strongly modifies the leverage angle of the tendon against the tibia at flexed angles (Fig. 7C). For convenience, the mechanical analogues of each FT joint are shown in Fig. 7C with the FTA set at 90 °; however, the FTA at which each muscle develops peak leverage (when θ, the shaded angle, is 90 °) will be offset by the above deviations for each moment arm. For all muscles except the metathoracic flexor, the tendon leverage will still vary sinusoidally with change in FTA; however Heitler's lump creates a complex variation in θ for the leverage developed by the metathoracic tendon as FTA changes.

The theoretical leverage curves for each muscle tendon are shown by the open symbols in Fig. 8 (for calculations, see Appendix). Note that the leverage of the metathoracic flexor increases nearly linearly as FTA decreases, and that peak leverage is developed at 0 ° FTA. The extensor muscles all show peak leverage at FTAs of less than 90 °; particularly the mesothoracic extensor, which has peak leverage at 55.6 °.

In principle, the torque developed on the tibia at tetanic muscle tension should vary with FTA according to the calculated leverage curves. This was observed, in general, for all muscles (except the metathoracic flexor), but the variation between preparations was high (Fig. 8, filled squares). The metathoracic flexor muscle showed a clear decrease in tension with decrease in FTA between 80 and 10 °, contrary to prediction.

In addition to leverage on the tibia being affected by the offset in the moment arm of each tendon, the length–tension characteristic of locust muscle would also offset the FTA at which peak force is developed against the tibia. The scant published data on locust muscle (Florey, 1968) suggest that active peak tension should occur slightly beyond rest length (RL) in the leg (approximately 110 % RL). This should shift the peaks in extensor tension to the left and the flexor peaks to the right of the predicted leverage peaks in Fig. 8. Only the pro- and mesothoracic extensor muscle curves seem to be shifted in the predicted direction.

Having characterised the mechanical leverage of each muscle at the femur–tibia joints, it is possible to compare these profiles (Fig. 8) with those of resistance reflex strength at different FTAs (Fig. 2). If the reflex actually compensates for the loss of leverage by increasing muscle firing at extreme angles, the histograms of Fig. 2 should be the inverse of the respective tension curves of Fig. 8. This expectation was only partially fulfilled, insofar as the general decrease in muscle tension is compensated by greater reflex output at FTAs smaller than that of peak tension (i.e. at FTAs to the left of the peak). Exceptions to this were the mesothoracic extensor muscle and the alternate reflex mode (filled bars)

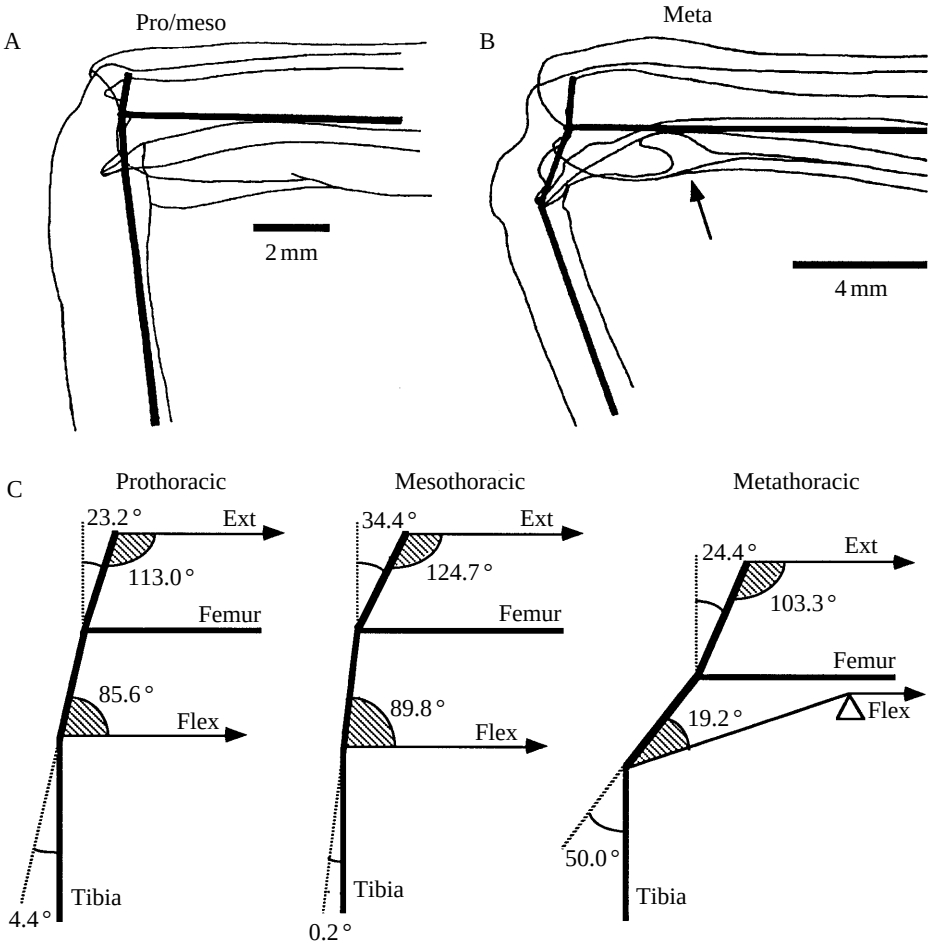

Peak leverage FTA		Peak leverage FTA		Peak leverage FTA	
Extensor	66.8 °	Extensor	55.6 °	Extensor	65.6 °
Flexor	85.6 °	Flexor	89.8 °	Flexor	0 °

Fig. 7. Mechanical configuration of the femur–tibia joints of locust legs. (A,B) *Camera lucida* drawings of a prothoracic/mesothoracic leg (A) and a metathoracic leg (B) cleared in lactophenol and stained with Lignin Pink, after KOH digestion. The pro- and mesothoracic legs appear essentially identical and have been drawn together. The heavy lines represent the axes of the femur and tibia and the projections from insertion points of the muscle apodemes to the joint pivot point. These projections represent the moment arms of the flexor and extensor muscle levers on the tibia. Heitler's lump is shown beneath the flexor apodeme in B (arrow). (C) Mechanical analogues of the femur–tibia joint levers at FTAs of 90 ˚ for the three legs, each based on measurements of six preparations. Although the diagrams depict the FTA at 90 ˚, at peak muscle leverage the FTA will be offset by the deviation (unshaded angle) of each moment arm from the tibial axis, for each particular muscle (given below each diagram), at which point the lever angle (shaded) will become 90 ˚. See Appendix for calculations.

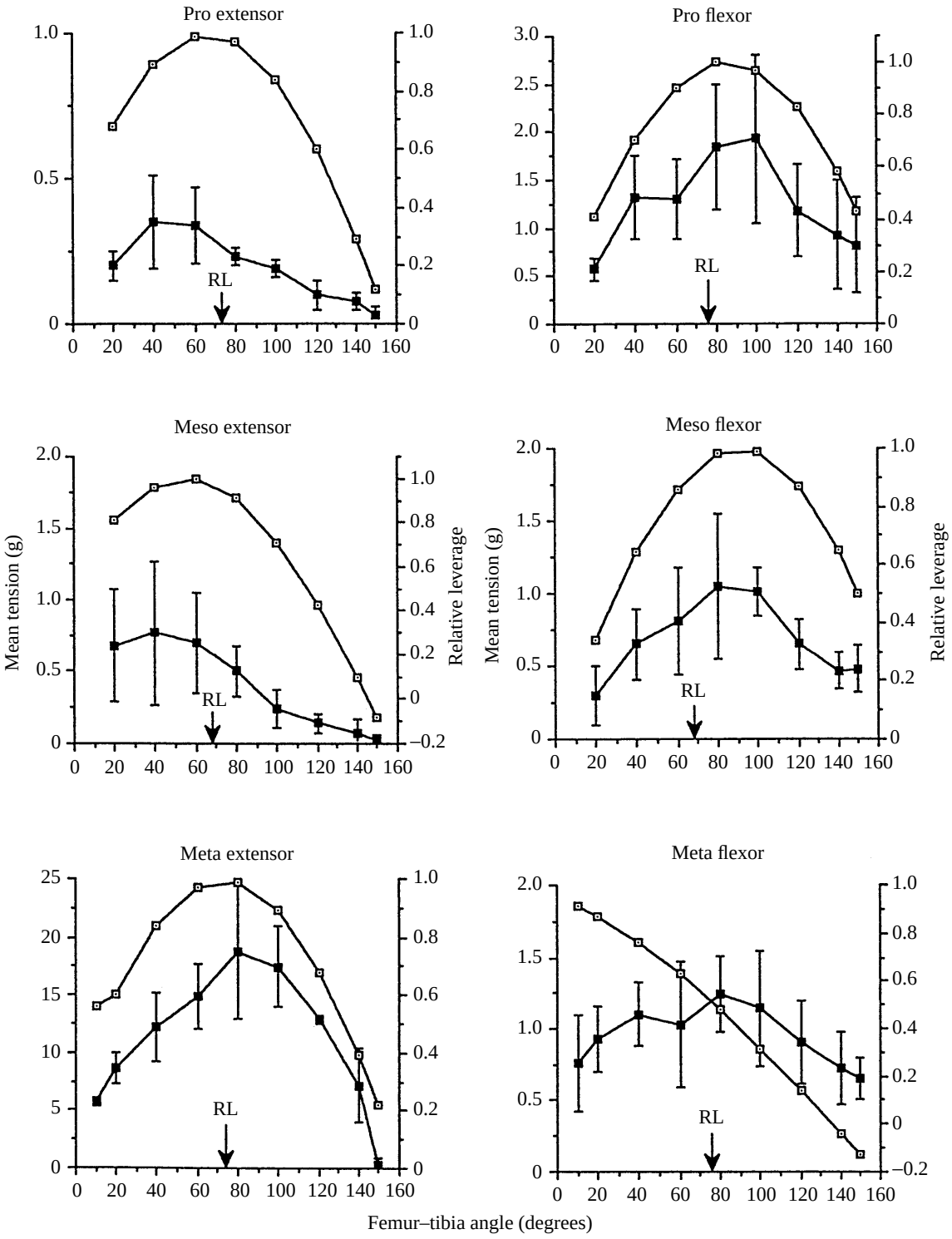
Pro extensor
Pro flexor
Meso extensor
Meso flexor
Meta extensor
Meta flexor
RL
Mean tension (g)
Relative leverage
Femur–tibia angle (degrees)

Fig. 8

Fig. 8. Variation in predicted leverage, and torque developed at tetanic muscle tension, at different FTAs for tibial extensor and flexor muscles. The relative leverage of each muscle (open symbols) theoretically varies as sinFTA, except for the metathoracic flexor, whose mechanics are complicated by Heitler's lump (see Appendix). However, the peak leverage of all muscles is offset from 90 ° FTA by the moment arm deviations given in Fig. 7. The torque on the tibia at tetanic tension (filled symbols) developed with motor nerve stimulation at various FTAs should, in principle, follow the relative leverage curves. Data are given as mean ± S.D. Sample sizes (*N*) are as follows: prothoracic extensor, 3; prothoracic flexor, 5; mesothoracic extensor, 6; mesothoracic flexor, 9; metathoracic extensor, 5; metathoracic flexor, 5. RL, mean muscle rest length FTA in locusts killed by cyanide (*N*=6).

plotted for the mesothoracic flexor (Fig. 2). The two histograms of these reflex strength data actually resembled the respective muscle tension curves rather than their inverse. For FTAs to the right of the tension peak, there is a decrease in reflex strength for all muscles, which would compound the effects of leverage loss, rather than compensating for these effects.

Discussion

We show for the first time that position-dependency of resistance reflexes occurs in all six legs of an insect and that it is likely to be a general property of arthropod postural systems. In view of this conclusion, surprisingly little attention has been devoted to its adaptive role in postural control. Bush (1962) suggested that, in crabs, it may serve primarily to restore the joint to a 'more suitable position' (in particular, to its resting mid-position) but he did not explore the adaptive consequences of this for postural control. A clear demonstration of position-dependency was shown in a further study of crab resistance reflexes by Spirito *et al.* (1972), but they did not discuss how this might be used by the animal. They did show, however, that resistance reflexes are unlikely to be used during walking in crabs, contrary to evidence in insects, where resistance (or, at least, negative feedback) reflexes play a role during the stance movement of the walking cycle (Bässler, 1967, 1983; Cruse and Pflüger, 1981), especially at higher velocities. In walking insects, the impact of position-dependent changes in the gain of resistance reflexes has not been explored, but it should present an interesting complication to the relative roles of these reflexes in prothoracic *versus* metathoracic leg control because stance and swing involve opposite movements in these legs. During the stance phase, the prothoracic leg flexes whereas the metathoracic leg extends, hence reflex gain would progressively increase during stance in the prothoracic leg but progressively decrease in the metathoracic leg (assuming reflex properties during walking are the same as during standing).

The reflexes characterised in the present report were primarily from slow motor neurones, which have thresholds low enough to be recruited by the relatively slow (1 Hz) tibial movements imposed. Higher velocities of movement should recruit faster motor neurones (Field and Burrows, 1982), but it is not known whether these have the same reflex characteristics, during standing and walking, as slow motor neurones.

Origin of position-dependency

The same position-dependent trend was observed at three sites in the resistance reflex

pathway: the motor neurones, the non-spiking interneurones and the FCO (Figs 3–5). Furthermore, the trend was common to motor neurones of both antagonistic muscles that move the femur–tibia joint. It seems clear that the origin of the effect lies in the phasic response sensitivity of the FCO. The effect could be due either (a) to a greater number of phasic neurones firing at flexed FTA arcs compared with the number firing at extended FTA arcs, or (b) to a greater synaptic efficacy for phasic neurones responding at flexed FTA movements than for the phasic neurones responding to movements at extended FTAs, given similar numbers of neurones in each population. Extracellular records from the FCO nerve (Fig. 5A) show that the former possibility is most likely. Similar results have been shown earlier by Field and Burrows (1982) (metathoracic FCO) and by Burns (1974) (mesothoracic FCO). Additional evidence for a greater number of flexed FTA phasic neurones comes from the intracellular studies of Hofmann *et al.* (1985) and Matheson (1990, 1992), all of which demonstrated a majority of phasic neurones with maximal sensitivities at small FTAs. For example, Matheson (1990) found 45 out of 72 extension-sensitive phasic neurones responding most strongly at angles close to 0 °, 22 with peak responses at mid-angles and three with peak responses near 120 ° (the remainder had bimodal response curves, with the major peak close to 0 °). For flexion-sensitive phasic neurones, 44 had peak responses close to 0 °, five had peak responses at mid-angles and three had peak responses near 120 °. We conclude that the total afferent synaptic drive onto the resistance reflex circuitry decreases as FTA increases to more extended angles.

Plasticity of the resistance reflex

Although the position-dependent characteristic appears to be hard-wired into the afferent side of the resistance reflex, there is now abundant evidence that the reflex can be modified during the transfer of FCO afference from spiking to non-spiking interneurones to motor neurones (Burrows *et al.* 1988). This may occur through graded changes in reflex gain or, apparently, through gating, as discussed below. Initial suggestions for plasticity came from extracellular studies of insect walking (Cruse and Pflüger, 1981; Bässler, 1983), which showed that the resistance reflex gain and the half-time of decay both decreased (to about 33 % in the stick insect) compared with their values in the inactive insect. Furthermore, the relative reflex strength of fast and slow extensor motor neurones reversed during walking (Cruse and Pflüger, 1981). Subsequent intracellular studies of interneurones have shown that responses of local spiking interneurones to FCO inputs, at the first stage of reflex integration, may be inhibited or suppressed by other afference (e.g. tarsal receptors) competing with that from the FCO (Burrows, 1988), or may be inhibited, suppressed or even reversed in sign when a competing motor programme (the ‘active response’) is activated in the animal (Bässler and Büschges, 1990).

Later in the resistance reflex pathway, non-spiking interneurones can increase or decrease the gain of the reflex onto motor neurones (Burrows *et al.* 1988; Büschges and Schmitz, 1991). These modifications may be caused by central pathways, such as descending input from the mesothoracic ganglion to non-spiking interneurones in the metathoracic ganglion (Laurent and Burrows, 1989*b*), or by direct peripheral afference from tactile receptors on the leg (Laurent and Burrows, 1988, 1989*a*). There is also

evidence that these gain changes are graded and may be compartmentalised within the non-spiking interneurones' branches (Laurent and Burrows, 1989*b*). Presumably the gain changes discussed so far are superimposed upon the position-dependency of the resistance reflex, although this point has not been tested. It should be noted that the resistance reflex pathway consists of parallel circuits, with FCO afference diverging even at the first level of interneurones (Burrows, 1988; Burrows *et al.* 1988), so that there is the possibility of wide variation in plasticity of the reflex and hence variation in the amount of position-dependency expressed at different points on the pathway.

Gating of the resistance reflex occurs when the central nervous system switches to alternative proprioceptive reflex modes. Zill and Jepson-Innes (1990) described a 'flexor mode' excitatory reflex which replaces the resistance reflex. It is restricted to flexor tibiae motor neurones and utilises FCO afference primarily at flexed angles in the locust hind leg. A similar 'active reaction' has been described in the stick insect (Bässler, 1988; Bässler and Büschges, 1990), in which the FCO afference appears to be gated away from the resistance reflex. When this occurs, a linear movement of the FCO apodeme causes an assistance reflex followed by a resistance reflex. It is not known whether the gain of the active reaction shows the kind of position-dependency observed in the resistance reflexes of the present study, although this is likely because the position-dependent character resides in the FCO.

Function of position-dependency in posture

A simple *a priori* model of postural control involving differential gain (position-dependency) in resistance reflexes might predict that the highest gain would occur at leg angles most often used in the resting posture. That is, a postural motor programme would set the legs to a preferred resting FTA, and thereafter resistance reflexes would automatically hold the legs locked at these angles against external perturbation. We tested this model by asking whether distributions of FTA (Fig. 6) matched the position-dependency of resistance reflexes in all six legs (Fig. 2). The comparison is complex because of differences among the three pairs of legs. No correlation is seen for the prothoracic legs. For the mesothoracic legs, the position-dependency profiles are unusual because they do not have a consistent peak gain at the smallest FTA, as seen for the other leg muscles. Thus, the resistance reflex profile of the mesothoracic tibial extensor roughly matches the preferred mesothoracic leg FTA profile (Fig. 6A), especially for vertical posture. A similar, but less convincing, match is seen for the alternative mode (filled bars in Fig. 2D) of the mesothoracic flexor muscle. For the metathoracic leg, the two kinds of plots roughly match, insofar as the peaks occur at small FTAs, especially for the vertical posture. The metathoracic flexor's lack of resistance reflexes beyond 80 ° is consistent with the metathoracic leg not being deployed beyond 95 ° at rest. The metathoracic extensor muscle does show significant reflex gain at larger angles, but this may be explained by the use of this leg in kicking and pushing behaviour, which may well use the FCO-mediated resistance reflex of this muscle to strengthen a push if an obstacle is encountered. We conclude that the reflex-mediated position-locking hypothesis may apply in the meso- and metathoracic legs, but that the main reason has to be found in another cause.

Our second hypothesis formulated to explain position-dependency predicted that changes in reflex gain would compensate for loss of muscle leverage at large and small FTAs. This would provide the animal with uniform leverage at all angles, if the plots of reflex position-dependency (Fig. 2) were the inverse of the generally sinusoidal leverage plots (Fig. 8). This clearly was not the case. Because the model only held true for angles less than 80–100 ° (approximately), we conclude that this is not a major role for position-dependency. Nevertheless, the compensation that does exist provides the animal with enhanced reflex strength at more flexed FTAs than would be the case if the FCO produced a uniform response at all joint angles. We propose below that the explanation for this enhancement lies in the mechanics of the insect's posture.

Consider an insect standing on a horizontal substratum (Fig. 9A), with its posture set to oppose the constant gravitational force, $\boldsymbol{g}$, using tonic motor drive onto the extensor muscles of the femur–tibia (F-T) joints. Any perturbance, H, in the horizontal plane will produce a torque at the F-T joint of a leg, equal to $\mathbf{x}(d)$ in Fig. 9B, where d is femur length and $\mathbf{x}$ is the vector component of force H perpendicular to the femur axis. For convenience, H is taken in the plane of the leg. In practice, because the legs are not all held normal to the body axis, any perturbing force in the horizontal plane will affect any given leg in proportion to the horizontal vector projection of that force along that leg's axis. The value of $\mathbf{x}$ varies sinusoidally with change in FTA and may be approximated by $\mathbf{x}=H\sin[(180-\mathrm{FTA})/2]$, as shown in the Appendix. The role of the resistance reflex is to oppose $\mathbf{x}$, thereby maintaining a stable posture. With an applied force H of 1.0 mN and d=10 mm, the calculated change in $\mathbf{x}$, as a function of FTA, is given by curve H (solid symbols) in Fig. 9C. This curve indicates that a given horizontal perturbation will exert a large torque onto the femur–tibia joint when the insect stands with the legs drawn in towards the body, i.e. at small FTAs. As the tarsi are placed farther away from the body, the FTAs will increase and the torque at the femur–tibia joint will decrease (Fig. 9C). It follows that, to maintain a stable posture against the force H, high gain will be required for resistance reflexes at small FTAs, but decreasing gain will be required for the reflexes as the FTA increases (i.e. as the legs become more spread, the posture will become inherently more stable because less and less torque will act on the femur–tibia joint).

The general trend of $\mathbf{x}$ in the above model agrees with the trends observed in the changes of resistance reflex gain at different FTAs (Fig. 2), although a sinusoid function, in particular, is not apparent in Fig. 2. We feel that, taken in conjunction with the preceding conclusions, this model offers a reasonable explanation of the role of position-dependency in resistance reflexes at the femur–tibia joint.

Some interesting consequences result from this analysis of resistance reflex gain at the femur–tibia joints. For example, any transient changes in vertical force $\boldsymbol{g}$ would produce a torque $\mathbf{x}(d)$ on the femur–tibia joint (as given in Fig. 9B), but the value of $\mathbf{x}$ would vary as the cosine of FTA. This would appear as curve G in Fig. 9C. It is immediately clear that the resistance reflexes in the tibial extensor muscles (Fig. 2A,C,E) are poorly prepared to cope with such perturbation if FTA exceeds 90–120 °. Indeed this may be why we observed modal FTAs of this or more flexed angles in our behavioural observations (Fig. 6). Presumably the insect experiences little change in $\boldsymbol{g}$ while at rest.

If an insect assumes a resting posture on a vertical surface, the above scenario reverses.

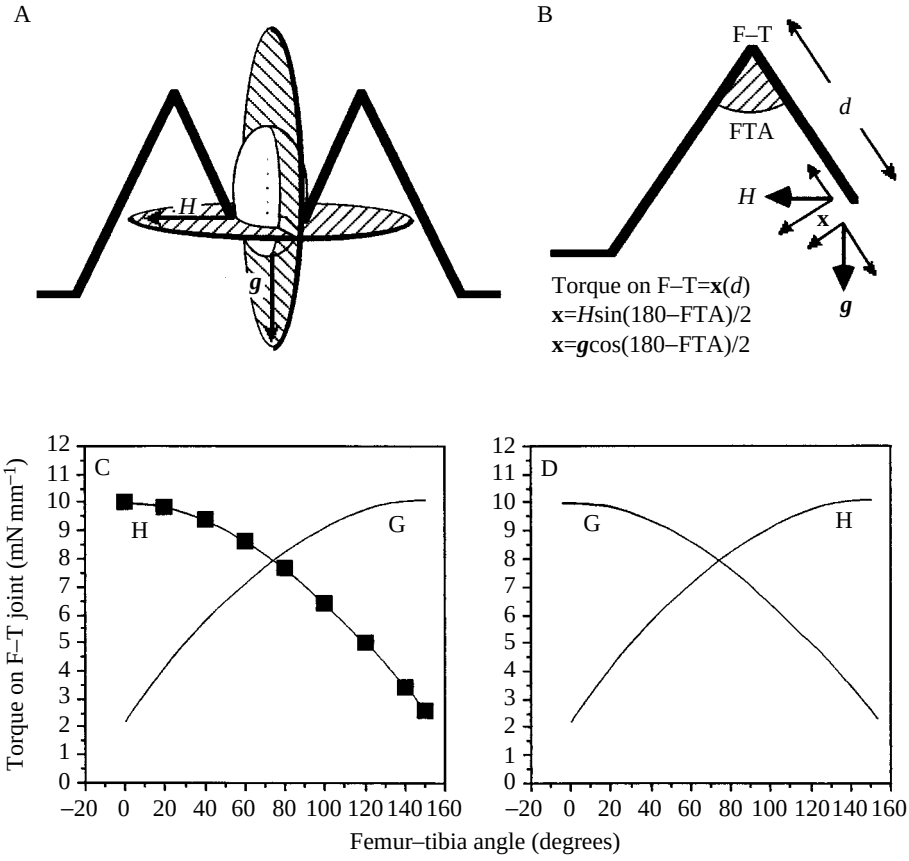

Fig. 9. Theoretical analysis of torque at the femur–tibia joint resulting from perturbation forces in the horizontal and vertical planes. (A) Model representation of a standing insect showing sites of action of horizontal force (*H*) and vertical (e.g. gravitational) force (***g***) on the legs. (B) Analysis of torque on the femur–tibia joint (F–T), produced by the moment arm **x**(*d*), which results from either horizontal or vertical forces. FTA, femur–tibia angle; *d*, length of femur; **x**, vector projection of *H* or ***g*** normal to the femur axis. (C) Variation in **x**(*d*) with change in FTA for an animal on a horizontal substratum. The torque resulting from a horizontal force of 1.0 mN (*d*=10 mm) is shown by curve H (filled symbols). The same force (***g***) exerted in the vertical plane (curve G) gives an increase in **x**(*d*) with an increase in FTA. Resistance reflexes could efficiently counter *H* but not ***g***. (D) For an animal resting on a vertical substratum, the model is rotated anticlockwise through 90° and the pair of curves becomes reversed. Now phasic changes in vertical force (***g***) can be efficiently resisted by the reflexes (curve G**)** but horizontal perturbations become less efficiently resisted as FTA increases (curve H).

Now the torque on the FT joints due to vertical forces, including gravity, varies as curve G in Fig. 9D, whereas the torque caused by forces in the horizontal plane (normal to the body axis) would be given by curve H. Because of the change in resistance reflex gain with change in FTA, vertical force perturbations may now be efficiently opposed, but the model predicts that horizontal perturbations may not be efficiently resisted at FTAs of

more than 90–120 ˚. In this respect, it is interesting to note that the meso- and metathoracic legs are held at smaller FTAs than those observed for posture on a horizontal surface (Fig. 6). In these legs, the tibial extensor muscles oppose ***g***, as in horizontal posture, and their resistance reflexes have high gain in the range of postural angles used on vertical substrata. However, the prothoracic legs resist gravity using the tibial flexor muscles when the locust is in vertical posture (facing upwards), whereas the tibial extensor serves this function in horizontal posture. Because the prothoracic flexor FTA tends to increase when the animal is in vertical posture, compared with horizontal posture (Fig. 6), it might appear that use of the resistance reflex is doubly disadvantaged for this muscle (based upon the above observations). However, this may not necessarily be important because the flexor can develop almost triple the peak force of the extensor in the prothoracic leg (Fig. 8) and its peak leverage is at a larger FTA (100 ˚) than that of the other tibial muscles. Hence, the prothoracic tibial flexors may be able to provide sufficient reflex strength even with these disadvantages.

The predicted low to intermediate gain for reflexes resisting horizontal forces while the animal is in a vertical posture is an interesting dilemma which deserves further

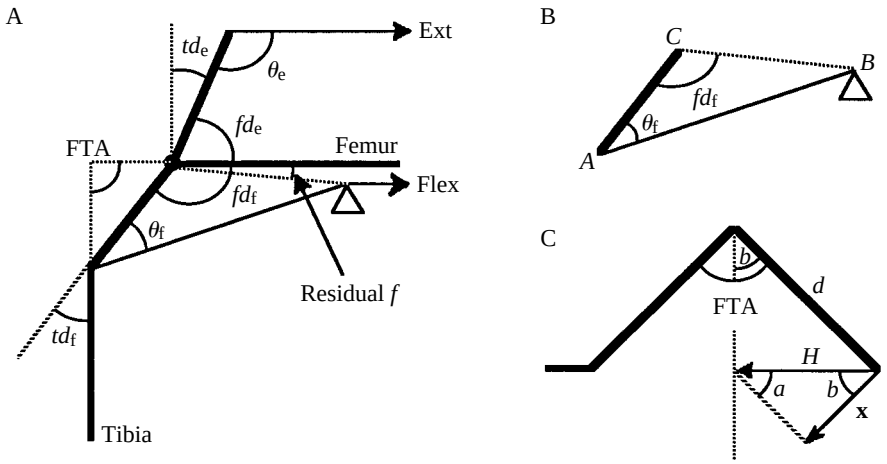

Fig. 10. Explanation of mechanical analysis of leverage and calculations of torque at the femur–tibia joint. (A) Mechanical analogue of muscle levers. Bold lines represent lever moment arms for the tibial extensor (Ext) and flexor (Flex) muscles as well as the axes of the femur and tibia. These moment arms are offset from the femur axis by angles fd_e and fd_f, respectively, and from the tibial axis by angles td_e and td_f, respectively. The angles of leverage are given by θ_e and θ_f, respectively. FTA, femur–tibia angle. The angle between the axis of the metathoracic femur and a line connecting the femur–tibia joint articulation to the apex of Heitler's lump (small triangle) is designated as residual *f*. It was used in calculating θ_f (see text). (B) Triangle *ABC*, extracted from the metathoracic leg analogue (A) and used to calculate θ_f. *A*, attachment point of flexor apodeme to tibia; *B*, apex of Heitler's lump; *C*, joint articulation. (C) Model used to calculate the relationship between FTA and **x**, the vector projection of horizontal force *H*, which exerts torque on the femur–tibia joint. The leg is assumed to form an isosceles triangle with the substratum, and FTA=2*b* (where *a* and *b* are the acute angles of the right-angled triangle, and *d* is length of the femur). See Appendix for calculations.

investigation. The insect may actually have weak resistance reflexes in this situation, in which case it may have little need to oppose large horizontal perturbations or it may employ additional reflex mechanisms unique to vertical posture. Alternatively, when the locust is on a swaying vertical stem, weak resistance reflexes may damp the rate of change in horizontal force experienced by the leg joints and reduce the chance that the tarsi would lose their grip. Strong resistance reflexes would keep the legs stiff and transfer more sudden shear forces to the tarsi, possibly causing slippage.

Appendix

Calculation of relative muscle leverage

Fig. 10 shows the relevant angles, measured from drawings of legs cleared and stained in lactophenol/Lignin Pink. The metathoracic leg is used as an example, since it includes the additional complications of Heitler's lump.

Ext and Flex are the directions of force exerted by extensor and flexor apodemes; θ_e and θ_f are the muscle tendon lever angle against the tibia for extensor (θ_e) and flexor (θ_f); fd_e and fd_f are the angles between the femur axis and the projection from the extensor (fd_e) and flexor (fd_f) tendon attachment points to the joint axis (refer to Fig. 7); td_e and td_f are the angles between the tibia axis and the above projections; and residual f is the angle between the femur axis and the line joining the joint axis to Heitler's lump.

Each extensor muscle leverage at any FTA is given by:

$$\sin\theta_e = \sin(\mathrm{FTA} + td_e)\,.$$

Pro- and mesothoracic flexor tibiae muscle leverage is given by:

$$\sin\theta_f = \sin(\mathrm{FTA} - td_f)\,.$$

Metathoracic flexor muscle leverage, $\sin\theta_f$ in Fig. 10, is calculated using measured distances for triangle *ABC* (Fig. 10B). From the Law of sines:

$$\sin\theta_f = [CB\sin(fd_f)]/AB\,,$$

where

$$fd_f = \mathrm{FTA} + td_f - \mathrm{residual}\ f$$

and, from the Law of cosines:

$$AB = \sqrt{(CB)^2 + (AC)^2 - 2(CB \times AC)\cos(fd_f)}\,.$$

The distances *CB* and *AC* remain constant as FTA varies, and hence may be measured directly.

The predicted FTA at which peak leverage (Fig. 7) occurs is found by setting θ to 90° and substituting mean *td* values measured from drawings. Hence, peak extensor leverage = $\sin(90 - |td_e|)$ and peak prothoracic and mesothoracic flexor leverage = $\sin(90 - |td_f|)$.

Peak metathoracic flexor leverage is found using triangle *ABC*, setting θ_f to 90°. From the Law of sines, find angle *B*, where:

$$\sin B = AC\sin\theta_f/CB$$

$$= 0.944\,.$$

Hence

$$B = 70.8^{\circ}.$$

Then find

$$fd_f = 180 - (B + \theta_f)$$

$$= 19.2^{\circ}.$$

Finally, these values are substituted into:

$$\text{FTA}_{(90^{\circ})} = fd_f - td_f + \text{residual } f$$

$$= 19.2 - 50 + 5.4$$

$$= -25.4^{\circ}.$$

However, because FTA cannot be less than 0°, maximum leverage occurs at the fully closed position (0°). At this position:

$$\theta_f = 90 - 25.4^{\circ}$$

$$= 64.6^{\circ}.$$

Derivation of torque exerted on femur–tibia joint

The model makes the simplifying assumption that the femur and tibia form an isosceles triangle with the substratum (Fig. 10C).

H is applied horizontal force; $\mathbf{x}$ is the projection of H perpendicular to the axis of the femur; d is the length of the femur; FTA is the femur–tibia angle; a and b are the acute angles of a right-angled triangle; and $\mathbf{x}(d)$ is torque.

To find $\mathbf{x}$:

$$\sin a = \mathbf{x}/H,$$

$$\mathbf{x} = H\sin a.$$

From a right-angled triangle:

$$b = 90 - a.$$

Since:

$$\text{FTA} = 2b$$

$$= 2(90 - a)$$

$$= 180 - 2a,$$

then

$$a = (180 - \text{FTA})/2$$

and, by substitution:

$$\mathbf{x} = H\sin[(180 - \text{FTA})/2].$$

Therefore:

$$\text{torque} = H\sin[(180 - \text{FTA})/2]d.$$

For force $\boldsymbol{g}$ (Fig. 9B), the vector projection is still $\mathbf{x}$, but:

$$\mathbf{x} = \boldsymbol{g}\cos a$$

by rotation through 90°.

Hence:

$$\text{torque} = \boldsymbol{g}\cos[(180 - \text{FTA})/2]d\,.$$

References

BÄSSLER, U. (1965). Propriozeptoren am Subcoxal- und Femur–tibia Gelenk der Stabheuschrecke *Carausius morosus* und ihre Rolle bei der Wahrnehmung der Schwerkraftrichtung. *Kybernetik* **2**, 168–193.

BÄSSLER, U. (1967). Zur Regelung der Stellung des Femur–tibia-Gelenkes bei der Stabheuschrecke *Carausius morosus* in der Ruhe und im Lauf. *Kybernetik* **4**, 18–26.

BÄSSLER, U. (1972). Der Regelkreis des Kniesehnenreflexes bei der Stabheuschrecke *Carausius morosus*: Reaktionen auf passive Bewegungen der Tibia. *Kybernetik* **12**, 8–20.

BÄSSLER, U. (1983). Neural basis of elementary behavior in stick insects. In *Studies of Brain Function*, vol. 10. Berlin: Springer-Verlag. 169pp.

BÄSSLER, U. (1988). Functional principles of pattern generation for walking movements of stick insect forelegs: the role of the femoral chordotonal organ afferences. *J. exp. Biol.* **136**, 125–147.

BÄSSLER, U. AND BÜSCHGES, A. (1990). Interneurones participating in the 'active reaction' in stick insects. *Biol. Cybernetics* **62**, 529–538.

BURNS, M. D. (1974). Structure and physiology of the locust femoral chordotonal organ. *J. Insect Physiol.* **20**, 1319–1339.

BURROWS, M. (1979). Graded synaptic interactions between local pre-motor interneurones of the locust. *J. Neurophysiol.* **42**, 1108–1123.

BURROWS, M. (1988). Responses of spiking local interneurones in the locust to proprioceptive signals from the femoral chordotonal organ. *J. comp. Physiol.* A **164**, 207–217.

BURROWS, M. AND HORRIDGE, G. A. (1974). The organization of inputs to motoneurones of the locust metathoracic leg. *Phil. Trans. R. Soc. Lond. B* **269**, 49–94.

BURROWS, M., LAURENT, G. AND FIELD, L. H. (1988). Proprioceptive inputs to nonspiking local interneurones contribute to local reflexes of a locust hind leg. *J. Neurosci.* **8**, 3085–3093.

BÜSCHGES, A. AND SCHMITZ, J. (1991). Nonspiking pathways antagonise the resistance reflex in the thoraco-coxal joint of stick insects. *J. Neurobiol.* **22**, 224–237.

BUSH, B. M. H. (1962). Proprioceptive reflexes in the legs of *C. maenas* (L.). *J. exp. Biol.* **39**, 89–106.

BUSH, B. M. H. (1965). Leg reflexes from chordotonal organs in the crab *Carcinus maenas*. *Comp. Biochem. Physiol.* **15**, 567–587.

CRUSE, H. AND PFLÜGER, H.-J. (1981). Is the position of the femur–tibia joint under feedback control in the walking stick insect? II. Electrophysiological recordings. *J. exp. Biol.* **92**, 97–107.

FIELD, L. H. (1991). Mechanism for range fractionation in chordotonal organs of *Locusta migratoria* (L.) and *Valanga* sp. *(Orthoptera: Acrididae). Int. J. Insect. Morph. Embryol.* **20**, 25–39.

FIELD, L. H. AND BURROWS, M. (1982). Reflex effects of the femoral chordotonal organ upon leg motor neurones of the locust. *J. exp. Biol.* **101**, 265–285.

FIELD, L. H. AND PFLÜGER, H.-J. (1989). The femoral chordotonal organ: a bifunctional orthopteran (*Locusta migratoria*) sense organ? *Comp. Biochem. Physiol.* **93**A, 729–743.

FIELD, L. H. AND RIND, F. C. (1977). The function of the femoral chordotonal organ in the weta. *N.Z. med. Jour.* **86**, 451.

FIELD, L. H. AND RIND, F. C. (1980). A single insect chordotonal organ mediates inter- and intra-segmental leg reflexes. *Comp. Biochem. Physiol.* **68**A, 99–102.

FLOREY, E. (1968). *An Introduction to General and Comparative Physiology*. Philadelphia: W. B. Saunders Co. 713pp.

HEITLER, W. J. (1974). The locust jump. Specialisation of the metathoracic femoral-tibial joint. *J. comp. Physiol.* **89**, 93–104.

HOFMANN, T., KOCH, U. T. AND BÄSSLER, U. (1985). Physiology of the femoral chordotonal organ in the stick insect *Cuniculina impigra*. *J. exp. Biol.* **114**, 207–223.

HOYLE, G. (1978). Distribution of nerve and muscle fibre types in locust jumping muscle. *J. exp. Biol.* **73**, 205–234.

LAURENT, G. AND BURROWS, M. (1988). Direct excitation of nonspiking local interneurones by exteroceptors underlies tactile reflexes in the locust. *J. comp. Physiol.* **162**, 563–572.

LAURENT, G. AND BURROWS, M. (1989*a*). Distribution of intersegmental inputs to nonspiking local interneurones and motor neurones in the locust. *J. Neurosci.* **9**, 3019–3029.

LAURENT, G. AND BURROWS, M. (1989*b*). Intersegmental interneurones can control the gain of reflexes in adjacent segments of the locust by their action on nonspiking local interneurones. *J. Neurosci*. **9**, 3030–3039.

MATHESON, T. (1990). Responses and locations of neurones in the locust metathoracic femoral chordotonal organ. *J. comp. Physiol*. **166**, 915–927.

MATHESON, T. (1992). Range fractionation in the locust metathoracic femoral chordotonal organ. *J. comp. Physiol*. **170**, 509–520.

MATHESON, T. AND FIELD, L. H. (1990). Innervation of the femoral chordotonal organ of *Locusta migratoria*. *Cell. Tissue Res*. **259**, 551–560.

SCHMITZ, J. (1985). Zur Systemanalyse des Coxa–Trochanter-Regellkreises der Stabheuschrecken *Carausius morosus*. *Verh. dt. Zool. Ges.* **78**, 241.

SPIRITO, C. P., EVOY, W. H. AND BARNES, W. J. P. (1972). Nervous control of walking in the crab, *Cardisoma guanhumi*. I. Characteristics of resistance reflexes. *Z. vergl. Physiol*. **76**, 1–15.

USHERWOOD, P. N. R., RUNION, H. I. AND CAMPBELL, J. I. (1968). Structure and physiology of a chordotonal organ in the locust leg. *J. exp. Biol*. **48**, 305–323.

WILSON, D. M. (1965). Proprioceptive leg reflexes in cockroaches. *J. exp. Biol.* **43**, 397–409.

WRIGHT, B. R. (1976). Limb and wing receptors in insects chelicerates and myriopods. In *Structure and Function of Proprioceptors in the Invertebrates* (ed. P. J. Mill), pp. 323–386. London: Chapman and Hall.

ZILL, S. N. (1985). Plasticity and proprioception in insects. I. Responses and cellular properties of individual receptors of the locust metathoracic femoral chordotonal organ. *J. exp. Biol*. **116**, 435–461.

ZILL, S. N. AND JEPSON-INNES, K. (1990). Functions of a proprioceptive sense organ in freely moving insects: characteristics of reflexes elicited by stimulation of the locust metathoracic femoral chordotonal organ. *Brain Res*. **523**, 211–218.